

An interpretation of wave refraction and its influence on foreshore sediment distribution

Vincent Jayaraj Jovivek^{1, 2*}, Nainarpandian Chandrasekar^{2, 4}, Ramakrishnan Jayangondaperumal³, Vikram Chandra Thakur³, Krishnan Shree Purniema¹

¹ Akshaya College of Engineering and Technology, Coimbatore 642109, India

² Centre for GeoTechnology, Manonmaniam Sundaranar University, Tirunelveli 627012, India

³ Structure and Tectonics Group, Wadia Institute of Himalayan Geology, Dehradun 248001, India

⁴ Francis Xavier Engineering College, Tirunelveli 627003, India

Received 21 March 2018; accepted 31 May 2018

© Chinese Society for Oceanography and Springer-Verlag GmbH Germany, part of Springer Nature 2019

Abstract

To analyze the grain size and depositional environment of the foreshore sediments, a study was undertaken on wave refraction along the wide sandy beaches of central Tamil Nadu coast. The nearshore waves approach the coast at 45° during the northeast (NE) monsoon, at 135° during the southwest (SW) monsoon and at 90° during the non-monsoon or fair-weather period with a predominant wave period of 8 and 10 s. A computer based wave refraction pattern is constructed to evaluate the trajectories of shoreward propagating waves along the coast in different seasons. The convergent wave rays during NE monsoon, leads to high energy wave condition which conveys a continuous erosion at foreshore region while divergent and inept condition of rays during the SW and non-monsoon, leads to moderate and less energy waves that clearly demarcates the rebuilt beach sediments through littoral sediment transport. The role of wave refraction in foreshore deposits was understood by grain size and depositional environment analysis. The presence of fine grains with the mixed population, during the NE monsoon reveals that the high energy wave condition and sediments were derived from beach and river environment. Conversely, the presence of medium grains with uniform population, during SW and non-monsoon attested less turbulence and sediments were derived from prolong propagation of onshore-offshore wave process. These upshots are apparently correlated with the *in situ* beach condition. On the whole, from this study it is understood that beaches underwent erosion during the NE monsoon and restored its original condition during the SW and non-monsoon seasons that exposed the stability of the beach and nearshore condition.

Key words: foreshore, grain size, wave refraction, sediment transport, beach, India

Citation: Jovivek Vincent Jayaraj, Chandrasekar Nainarpandian, Jayangondaperumal Ramakrishnan, Thakur Vikram Chandra, Shree purniema Krishnan. 2019. An interpretation of wave refraction and its influence on foreshore sediment distribution. Acta Oceanologica Sinica, 38(5): 151–160, doi: 10.1007/s13131-019-1446-y

1 Introduction

The waves and wave induced currents are the primary sea undulations that lead to the sediment transportation in the nearshore region. The direction of wave propagation depends on the seabed topography. The uneven nearshore topography influences wave celerity, breaking wave height and direction and thus the direction of the wave approaching the coast is altered. Therefore, the waves undergo refraction and tend to become normal to the shoreline. This phenomenon is called wave refraction (Kirby and Dalrymple, 1994; López-Ruiz et al., 2015). Munk and Traylor (1947) provided a detailed mathematical structure for constructing wave refraction and discussed the wave refraction impact on nearshore process. Followed by this, many researchers used computer based wave refraction models to examine the physical process of different types of coasts (Shepard and Inman, 1950; Harrison and Wilson, 1964; Orr, 1969; Skovgaard et al., 1975; Jing and Massel, 1994; Mathiesen, 1987; Kirby and Dalrymple, 1994; López-Ruiz et al., 2015; Jovivek and Chandrasekar, 2016). From these studies, it is understood that four oceanographic parameters namely seabed topography, wave period, direction of wave approach the coast and deep-water wave height are the key para-

meters for constructing wave refraction diagram. In general, wave refraction helps to understand the wave process and the depositional environment at a particular region. Even though, quite a lot of papers had provided the spatial relationship between wave refraction and sediment distribution (Angusamy et al., 1998; Bird, 2000; Kunte et al., 2001; Short, 2006; Amrouni-Bouaziz et al., 2007; Soomere et al., 2008; Yates et al., 2011; Jovivek and Chandrasekar, 2014, 2017; Segtnan, 2014; Saravanan and Chandrasekar, 2015), this particular study provides a comprehensive view of the physical impact of wave refraction on grain size and depositional environment in accordance to the varying monsoonal condition.

In this research, about ten beaches were chosen between Thirukadaiyur and Velankanni along the central Tamil Nadu coast, India (Fig. 1). This area is mainly composed of the coastal plain, fringing the Eastern Ghats with varying altitude of 75 to 105 m. As majority of these coastal plain forms a part of the Cauvery delta, a thick cover of alluvium is commonly observed (Jovivek and Chandrasekar, 2014, 2017). Beaches are found to be in semi-diurnal tidal condition with mean high tide of 0.68 m and mean low tide of 0.28 m (Chart No. 3007, scale 1: 35 000, Year 2010,

*Corresponding author, E-mail: vjovivek@gmail.com

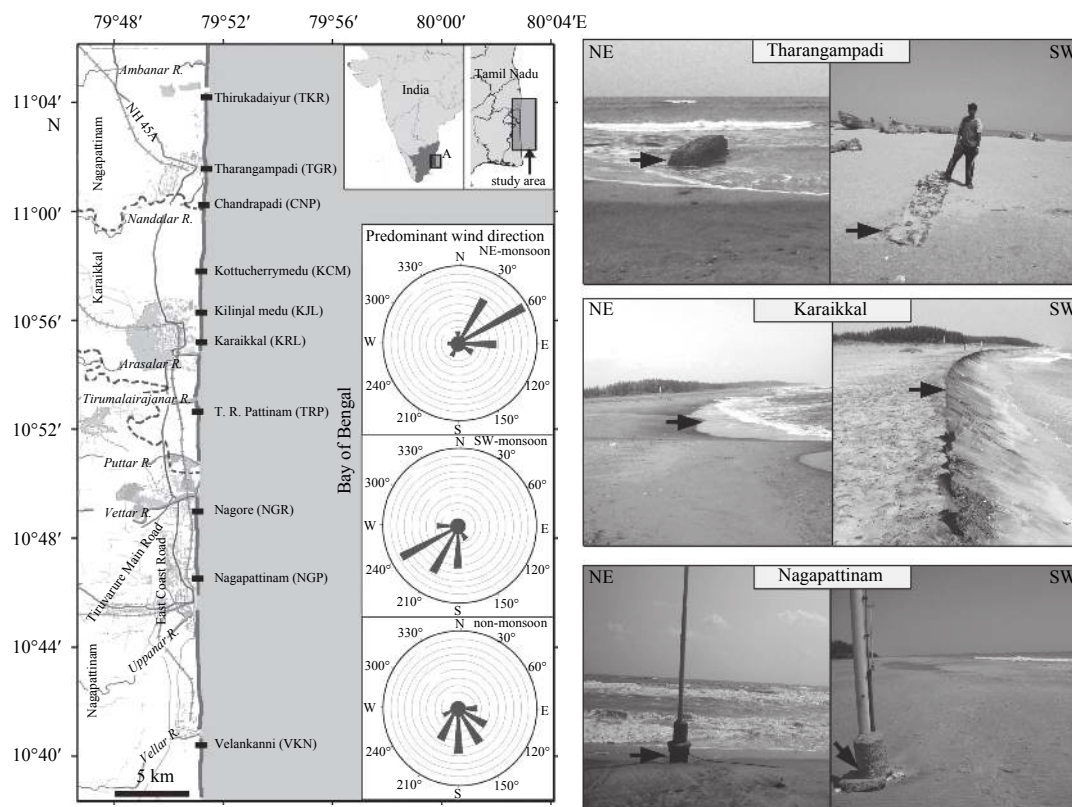


Fig. 1. Location map of the study area. The wind rose diagram depicts predominant wind direction prevailed in the coast. The field photographs illustrate beach morphodynamic condition with respect to the NE and SW monsoon condition.

published by NHO, Dehradun). Wind speed is normally ranging between 11 to 26 km/h and the speed is observed to exceed 50–75 km/h during the storm/tropical cyclone condition. The corresponding study area encloses some of the major rivers namely Ambanar and Nandalar in the north, Arasalar, Tirumalaivajana, Puttar and Vettar in the central part and Uppanar and Vellar in the south. Majority of the subsurface water is consumed by the industries along the coastal regions, which is found to be a developing threat, apart from other threat caused by the industries. In addition to this, lowering of water levels below mean sea level is observed throughout the year due to the influence of natural and man-made activities. According to the Central Ground Water Board, Chennai-2011, the quality of the ground water in eastern and southeastern parts is insufficient. The cultivation of Paddy these regions has resulted in the extraction of the water from the aquifer and the fertilizers used for this purpose has also affected the medium. Mangroves are found to appear on the high tidal mudflats near the Karaikkal coast. The coastal stretch includes backwaters, salt pans, several distributaries channels, two fishing harbors and one port.

The northeast (NE) monsoon (October to January), southwest (SW) monsoon (June to September) and non-monsoon (February to May) are the three seasons, that is experienced by the study area, in a year. Though there were no official bounds, the formation of cyclones typically formed between May and December, with the peak from October to December along the east coast of Tamil Nadu. An analysis of the frequency of cyclones on the East coast of India between 1891 and 1995 shows 449 cyclones and 189 severe cyclonic storms occurred in and around east coast stretch which indicates that a moderate to severe cyclone hits the Tamil Nadu coast every two years during the NE monsoon. Re-

cently, tropical cyclones such as Thane (2011), Nilam (2012), Kyant (2016), Nada (2016), Vardah (2016) and Ockhi (2017) creates severe damage along the central Tamil Nadu coast. However, there is no significant storm effect found in the SW and non-monsoon seasons. It shows that formations of cyclones in these regions are strongly related to the seasonal migration of Inter Tropical Convergence Zone (ITCZ) (Dube et al., 1997).

2 Data and methods

The major parameters needed for the construction of wave refraction diagram is wave direction (angle in $^{\circ}$), wave period (s), deep-water wave height (m) and bathymetry data. The wave period and the direction of wave approach the coast are obtained from the field observation. The field data is collected from 2011 till 2013 on a monthly and seasonal basis. From the field data, we observed that wave condition and grain size variations are stable for three years. Hence, we used the seasonal data of one year, instead of entire dataset (20 January 2011 (NE monsoon), 17 May 2011 (non-monsoon) and 12 September 2011 (SW monsoon)). The wave period is obtained by observing the time taken by waves for passing two successive crests at a fixed point. Thus the predominant high and low wave period is estimated from the observation of 300 successive waves. The direction of wave approach, along the coast is measured by observing the average direction of a floating buoyant plate at breaker zone within 30 minutes time period. The deep-water wave height is obtained from the wave atlas of the Indian coast (Chandramohan et al., 1990). The bathymetry of the present study region is extracted from Global 30 Arc-Second Elevation Data Set (GTOPO30). The wind and tide data were obtained from the online resource (<https://www.windfinder.com/>).

The wave refraction diagram for different monsoon seasons is created with the help of the computer program, the Ocean Wave Tool (ONWET). This software is exclusively designed for the beach morphology and wave analysis. This tool is mainly deployed in order to perform the special temporal analysis of beach profile, empirical orthogonal function (EOF) analysis, wave refraction analysis and quantifying sediment transport rate. This software is a window based application which is compiled under the Matlab environment. The outcome of the ONWET is reliable with the widely accepted wave refraction tools (Joevivek and Chandrasekar, 2016).

The beach and wave classification has been carried out by using breaking wave type and beach morphodynamic state model. Galvin (1968) proposed a semi empirical formula to estimate breaking wave type:

$$\zeta = \frac{\tan\beta}{(H_b/L_0)^{0.5}}, \quad (1)$$

where H_b is breaking wave height, L_0 is deep water wavelength, and β is foreshore slope ($^\circ$). The data of breaking wave height and foreshore slope for the entire study area is shown in Table 1.

Similarly, morphodynamic state of beach system can be calculated based on Wright and Short's morphodynamic state model (Wright and Short, 1984):

$$\Omega = \frac{H_b}{w_s T}, \quad (2)$$

where w_s is the particle settling velocity and T is the wave period.

The results of breaking waves and morphodynamic state are classified into three domains (Short, 2006). The breaking wave type is classified as surging breakers, plunging breakers and spilling breakers. If $\zeta > 2$, it is a surging breakers. If ζ is between 0.4 and 2, it is a plunging breakers, and if $\zeta < 0.4$, it is a spilling breakers. Similarly, beach morphodynamic state can be categorized as reflective, intermediate and dissipative. If $\Omega < 1$, it is a reflective beach. If Ω is between 1 and 6, it is an intermediate beach and if the value of $\Omega > 6$, it is a dissipative beach.

The foreshore (swash zone) is the zone of land-water interaction and hence it is considered to be a major dynamic region. Therefore, sediment samples were collected from the foreshore region during the spring low tide. The precise region, from which the sample is obtained, is shown in Table 1. Aluminum grabber was used to collect surface sediments; it is properly labeled and taken to laboratory for grain size analysis. About 100 g were collected from each sample with the help of the coning and quartering method. These collected samples were further pre-treated through the following chemical processes. Initially, the clay fractions were removed by shuffling in the fresh water. Further, organic, inorganic contents and fine broken shells were removed by the addition of 6% H_2O_2 , followed by the addition of 10% of HCl. The size of the pre-treated sediments was categorized based on the report of Wentworth (1922). A mechanical sieve shaker with quarter Φ interval from +40 to +230 ASTM units was used for sieving the pre-treated samples. The logarithmic method of moments was used to evaluate the statistical measure of sieve fractions as it produces a better reliable outcome, compared to that of the arithmetic, geometric and graphical measures (Blott and Pye, 2001). Further, depositional environment of the beach sediments were examined by traditional methods namely, bi-varient plot (Friedman, 1967; Moiola and Weiser, 1968), Visher plot or

log-normal distribution curve (Visher, 1969) and CM diagram (C is the coarsest one percentile and M is the median grain size) (Passega, 1964).

3 Results and discussion

3.1 Wave refraction

The physical behavior of the waves is exhibited by wave refraction pattern, when these waves propagate from deep to shallow region. When waves enter the breaker zone, undertow current is interrupted by the sea bed. Hence wave speed and wavelength decreases while wave period remains constant (Davidson-Arnott and Greenwood, 2009; Masselink and Puleo, 2006). The direction of waves at breaker zone tends to become parallel to the shoreline, which creates refraction depending upon the bottom topography. Figure 2 illustrates elevation profile of seabed topography at 5 m interval contours. This figure shows the existence of a uniform and even seafloor in the northern part and a non-uniform and uneven seafloor in the central and southern part. The arrows represent the actual direction of wave approach, in the coast during different seasonal conditions. According to the traces of bottom topography the deep water waves are observed to approach the coast 45° (from NE to SW) during the NE monsoon. The contour traces along this direction reveals that the sea bed is relatively steady from the deeper to the shallow water region. On the other hand, deep water waves approach the coast at 135° from SE to NW direction and the contour traces along this direction reveals an uneven sea bed condition. During the non-monsoon period, the waves were observed to attain a calm condition and the direction of wave approach on the coast was observed to be at 90° (from E to W), almost normal to the shoreline.

The refraction patterns of wave approach at 45° in the wave period (T) of 8 and 10 s reveals a series of convergence zone at breaking point (Fig. 3). This convergence leads an increase in the wave height or energy that causes foreshore erosion (Fig. 1). During this period, the sediments are eroded by uprush and it is carried by back wash, towards surf zone (Joevivek and Chandrasekar, 2014, 2017). Due to collision between backwash and shoreward successive spilling breakers, the eroded sediments are formed as the sandbars in the surf zone (Table 1). In addition to that, almost all the river mouths in the study area reveal a convergence towards the shoreline, due to the presence of a shoal at the adjacent shoreface. The refraction patterns for 135° in a wave period of 8 and 10 s have shown a slight divergence pattern in the shoaling zone (Fig. 3). The presence of the sea bed topography at this position is uneven, as the wave rays diverge during the SW monsoon. Divergence reduces wave heights or energy that results in accretion or deposition. Therefore, the waves approaching the coast appeared to be surging breakers with calm condition at a constant wave period and with small amplitude (Table 1). In this process, sediments get deposited in the foreshore region; the heavies get settled at the beginning of the divergence zone and the lighter minerals get settled in the forth-coming stages (Fig. 1). The refraction patterns at 90° and $T=8$ and 10 s are almost similar and orthogonal to the shoreline (Fig. 3). During the process, the sandbars are destroyed by the plunging and collapsing breakers and it is further transported by onshore-offshore sediment transport (Joevivek and Chandrasekar, 2014, 2017).

3.1.1 Impact on grain size distribution

The textural results reveals that the foreshore sediments are mostly composed of medium to fine sand ($1.71\Phi-2.09\Phi$), moder-

Table 1. Grain size, beach and wave morphology along the entire study area during the different monsoonal condition

		Sampling site and geo-coordinate (stations from north to south, see Fig. 1)											
Grain size and wave morphology		TKR 11.073°N, 79.857°E	TGP 11.024°N, 76.856°E	CNP 11.002°N, 79.855°E	KCM 10.964°N, 79.854°E	KJL 10.940°N, 79.853°E	KRL 10.918°N, 79.853°E	TRP 10.883°N, 79.852°E	NGR 10.813°N, 79.851°E	NGP 10.787°N, 79.851°E	VKN 10.676°N, 79.854°E		
NE monsoon													
Grain size parameters													
Mean (Φ)		2.06	2.07	2.06	2.06	2.07	2.08	2.07	2.09	2.09	2.11		
Sorting (Φ)		0.57	0.58	0.53	0.55	0.58	0.58	0.57	0.58	0.58	0.67		
Skewness (Φ)		1.13	1.11	1.12	1.12	1.09	1.06	1.08	1.00	1.00	0.94		
Kurtosis (Φ)		2.92	2.89	2.90	2.93	2.86	2.79	2.89	2.69	2.71	2.59		
Beach & wave parameters													
Breaking wave height/m		0.88	0.82	0.74	0.94	0.88	0.83	0.92	0.92	0.98	0.70		
Foreshore slope/(°)		1.80	1.60	1.50	1.40	1.60	1.70	1.60	1.90	1.90	2.0		
Beach morphodynamic state		dissipative	dissipative	dissipative	dissipative	dissipative	dissipative	dissipative	dissipative	dissipative	dissipative		
Breaking wave type		spilling	spilling	spilling	spilling	spilling	spilling	spilling	spilling	spilling	spilling		
Mean wave direction/(°)		45	45	45	45	45	45	45	45	45	45		
Tide (high/low)/m		0.72/0.06	0.69/0.09	0.73/0.08	0.71/0.07	0.73/0.05	0.75/0.08	0.72/0.09	0.77/0.08	0.73/0.08	0.71/0.09		
SW monsoon													
Grain size parameters													
Mean (Φ)		1.79	1.8	1.79	1.80	1.79	1.81	1.85	1.86	1.86	1.85		
Sorting (Φ)		0.35	0.36	0.32	0.35	0.37	0.36	0.39	0.34	0.35	0.37		
Skewness (Φ)		2.47	2.39	2.40	2.37	2.39	2.23	1.95	1.85	1.85	1.89		
Kurtosis (Φ)		8.75	8.30	8.41	8.31	8.46	7.55	6.10	5.63	5.71	5.91		
Beach & wave parameters													
Breaking wave height/m		0.48	0.67	0.49	0.46	0.42	0.68	0.38	0.41	0.53	0.46		
Foreshore slope/(°)		9.78	10.49	10.44	9.45	9.31	10.51	11.51	10.82	10.79	9.64		
Beach morphodynamic state		reflective	reflective	reflective	reflective	reflective	reflective	reflective	reflective	reflective	reflective		
Breaking wave type		surging	surging	surging	surging	surging	surging	surging	surging	surging	surging		
Mean wave direction/(°)		135	135	135	135	135	135	135	135	135	135		
Tide (high/low)/m		0.94/-0.08	0.92/-0.09	0.91/-0.12	0.88/-0.13	0.92/-0.09	0.94/-0.08	0.92/-0.13	0.87/-0.14	0.89/-0.17	0.91/-0.15		
Non-monsoon													
Grain size parameters													
Mean (Φ)		1.91	1.92	1.92	1.92	1.93	1.94	1.93	1.95	1.95	1.98		
Sorting (Φ)		0.47	0.46	0.47	0.48	0.49	0.47	0.42	0.44	0.45	0.49		
Skewness (Φ)		1.69	1.65	1.67	1.64	1.61	1.55	1.55	1.45	1.44	1.36		
Kurtosis (Φ)		4.71	4.58	4.66	4.57	4.50	4.30	4.33	4.00	4.00	3.72		
Wave parameters													
Breaking wave height/m		0.68	0.72	0.70	0.74	0.78	0.68	0.75	0.74	0.86	0.67		
Foreshore slope/(°)		4.62	3.35	4.51	3.40	3.08	4.24	3.12	4.18	3.24	4.42		
Beach morphodynamic state		intermediate	intermediate	intermediate	intermediate	intermediate	intermediate	intermediate	intermediate	intermediate	intermediate		
Breaking wave type		plunging	collapsing	collapsing	plunging	plunging	plunging	collapsing	collapsing	plunging	collapsing		
Mean wave direction/(°)		90	90	90	90	90	90	90	90	90	90		
Tide (high/low)/m		0.82/0.15	0.89/0.16	0.83/0.19	0.81/0.17	0.84/0.21	0.82/0.18	0.85/0.19	0.87/0.16	0.83/0.18	0.81/0.19		

Note: TKR represents Thirukadaiyur, TGP Tharangampadi, CNP Chandrapadi, KCM Kottucherry, KJL Kilinjil medu, KRL Karaikal, TRP T. R. Pattinam, NGR Nagore, NGP Nagapattinam, and VKN Velankanni.

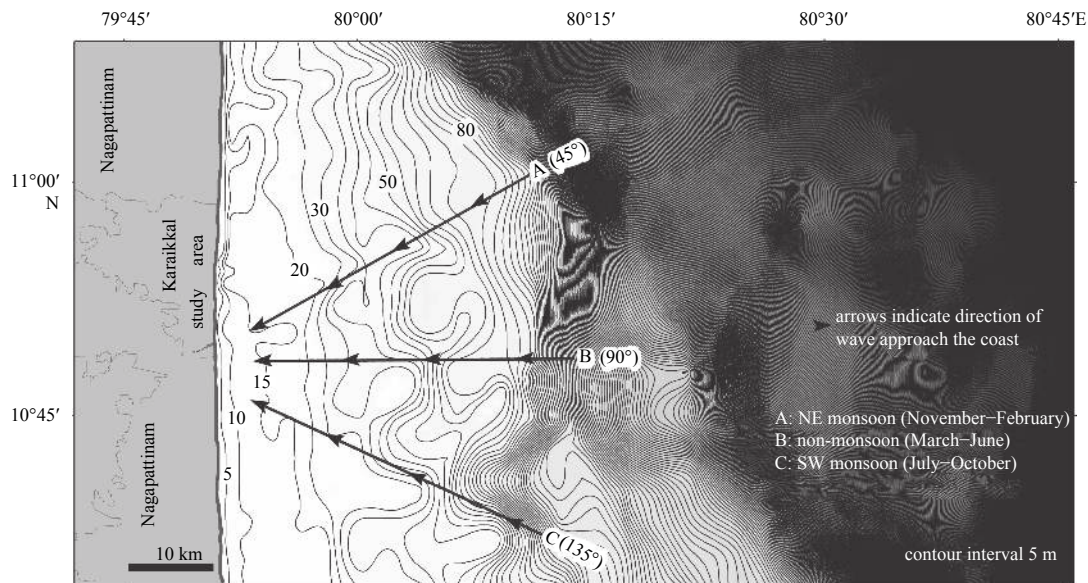


Fig. 2. Sea bed bottom topography of the study area is represented by the contour lines with 5 m interval. The arrow indicates direction of the wave approach the coast.

ately to very well sorted (0.67Φ – 0.44Φ), fine skewed to very fine skewed (1.0Φ – 2.47Φ) and mesokurtic to very leptokurtic (2.71Φ – 8.75Φ) (Table 1). The mean value reflects the average size distribution that was influenced by the source of supply or environment of deposition. Figure 4 shows the grain size distribution and cumulative distribution of the sediment samples. The frequency curve plot shows the presence of bi-model grain size distribution in the coast. The first population peaked at 2Φ and the second population peaked at 3Φ . The first population increase from NE to SW monsoon clearly reflects the seasonal wave condition. During the SW and non-monsoon season, the medium size fraction tends to be highly populated as the sediment supplied by the swash zone possesses low wave energy. Conversely, during the NE monsoon the second population reveals comparatively higher peak of the fine population which is probably due to the fluvial action along with active erosion of beach terrace. The cumulative plot shows the existence of similar grain size population in the entire study area. As observed, the NE monsoon displays a cumulative distribution blend of medium and fine sands. This is due to the sediments that were derived from mixture of wave and fluvial processes. However, in SW and non-monsoon season, medium sand is dominated as compared to fine sand. This is due to the sedimentation process that takes place by suspension process in calm wave condition.

During the NE monsoon, the majority of the sediments are fine grained with mixed population due to the influx of sediments by river discharge. In contrast, during the SW and non-monsoon seasons, sediments are medium grained with uniform population due to the continuous process of longshore sediment drift (Joevivek et al., 2018a). The variations observed in sediment sorting shows the nature of the wave energy and sediment transport, prevailed in the coast. Lesser sorting values denotes that sediments are better sorting by prolong transportation processes (Briggs, 1977; Dyer, 1986; Folk and Robles, 1964). During the SW monsoon, the study area accomplished less sorting values which indicates deposition caused by the onshore–offshore sediment transport. During the NE monsoon, coast experienced moderate sorting values that indicate moderately well sorted condition. The confluence of river mouth brought unconsolidated sedi-

ments, during the rainy season and therefore river sediments gets mixed with the offshore sediments which tends to reduce sorting nature.

From an entire study period, sediments reveals positive skewness which indicates that foreshore region had influenced fine skewed to very fine skewed conditions. The positive or negative sign of skewness indicate high or less wave energy conditions (Martins, 1965; Friedman, 1961; Duane, 1964). During the SW monsoon, sediments reveal a positive with very fine skewness that indicates continuous process of sediment deposition over a low energy wave condition. During the NE monsoon, the sediments became fine skewed (that is nearly symmetrical distribution), indicates the mixture of fluvial and beach sediments. The Kurtosis analysis shows that sediments are observed to be in mesokurtic to very leptokurtic nature. Higher kurtosis value revealed better sorting process while lower kurtosis value revealed poor sorting nature (Boggs, 2009). In this study, higher kurtosis value (leptokurtic to very leptokurtic) is noticed during the SW monsoon. It is due to the fact that, divergence waves produce better sorting by low energy wave propagation. During the NE monsoon, sediments attained lesser kurtosis value (mesokurtic) which indicates that, high energy waves leads to transport of river and beach sediments.

3.1.2 Impact on sediment depositional environment

The bivariate plot shows distinction within the group of samples of the entire coast with respect to the seasonal variation (Fig. 5a). The standard deviation against inclusive skewness indicates that moderately well sorted with fine skewed sediments are mostly of river and beach environments and well sorted with very fine skewed sediments are mostly of beach environment (Friedman, 1961). During the NE monsoon, convergence of waves influence suspended sediment transport of sediments present in the nearshore bed and adjacent to the river mouth. This causes mixture of sediment distribution and hence the source of deposition is mostly of river and beach. In contrast, during the SW and non-monsoon, divergence and calm waves produce the well sorted reworking of sediments by wave processes and therefore source of deposition belongs to the beach

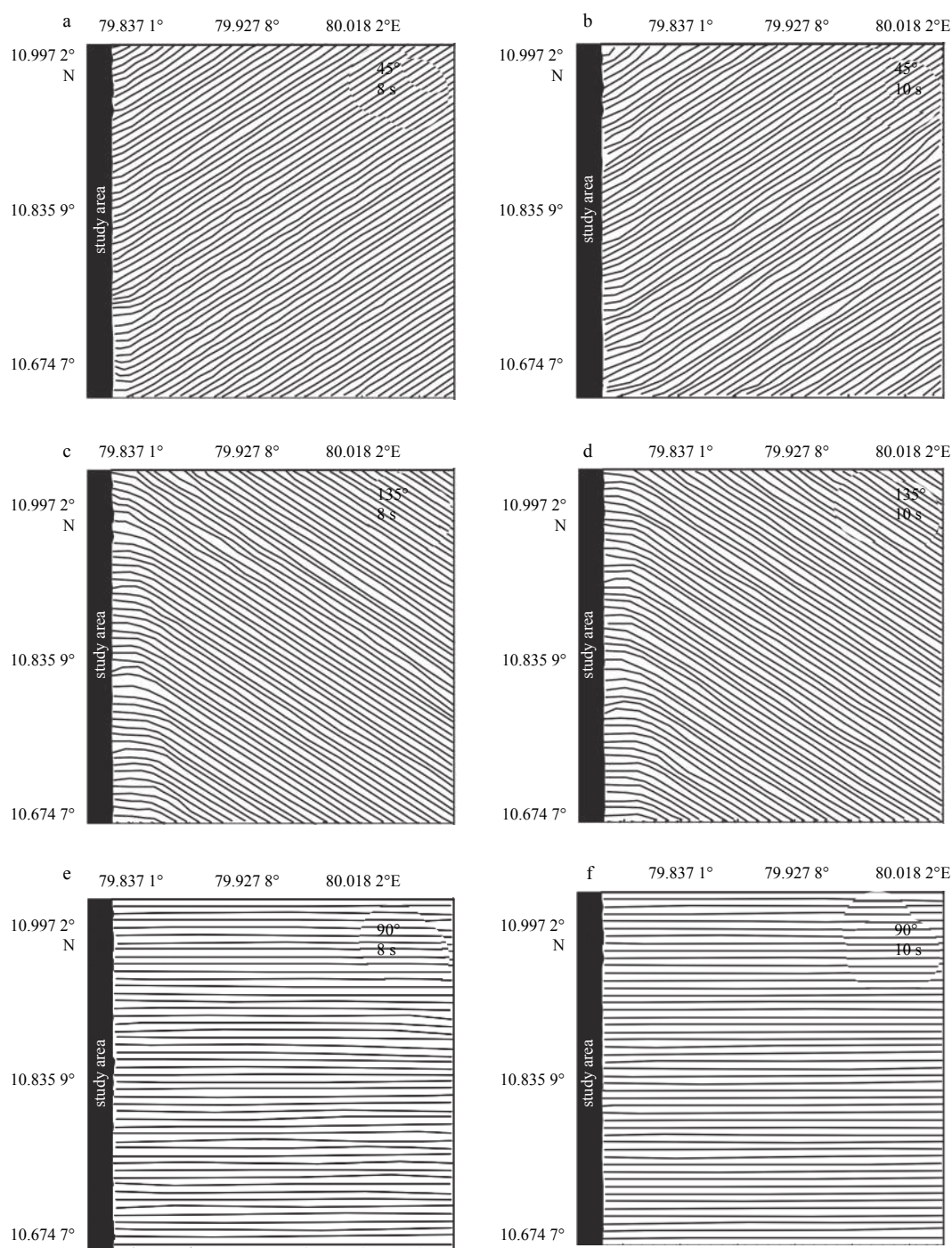


Fig. 3. Wave refraction diagram for the different seasonal condition. a and b. Refraction patterns of wave approach the direction of 45° and wave period (T) of 8 and 10 s, c and d. Refraction patterns of wave approach the direction of 135° and wave period (T) of 8 and 10 s, and e and f. refraction patterns of wave approach the direction of 90° and wave period (T) of 8 and 10 s.

environment.

As seen in the Visser plot (Fig. 5b), a well-developed suspension population noticed during the NE monsoon, while less suspension noticed during the SW monsoon. The presence of a suspension population and the truncation of the coarse population account for the positive skewness characteristic of foreshore deposits (Visser, 1969). The high suspension population during NE monsoon indicates high energy conditions, thereby depositing finer particles and the discharge of sediments by river and beach.

The grain size ranging from 1.25Φ to 2.25Φ falls under the traction population. The truncation between saltation and suspension within the range of 2.25Φ to 3.25Φ . The slope of saltation population is high during NE monsoon as compared to the SW monsoon. It reveals moderately well sorted saltation population and poorly sorted suspension population and implies that sediments are fluvial type (Angusamy and Rajamanickam, 2006). The gentle slope of saltation during SW monsoon, accomplished the deposition of suspended sediments and sand movement due to

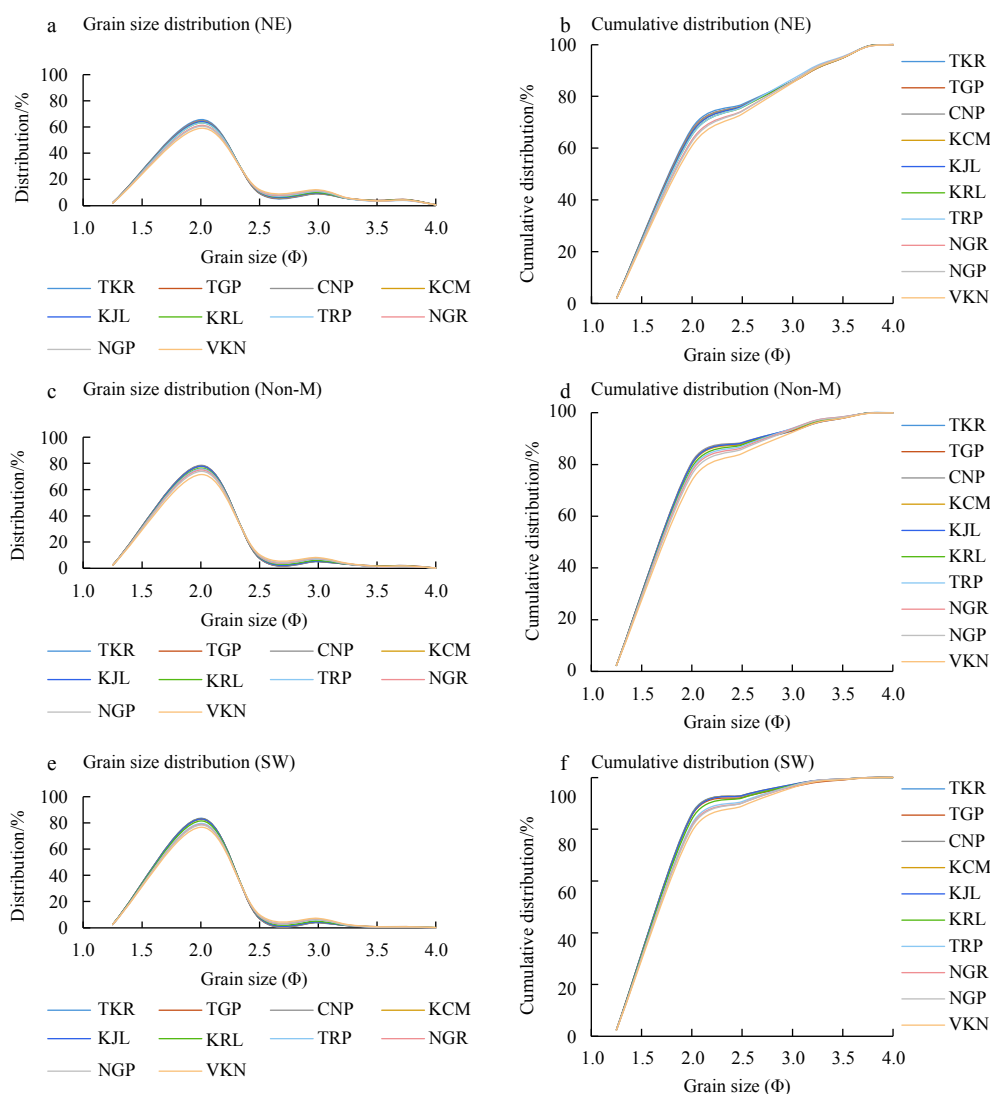


Fig. 4. Grain size and cumulative distribution in different seasons. a and b. Northeast (NE) monsoon (January 2013), c and d. non-monsoon (Non-M) season, and e and f. southwest (SW) monsoon. Stations: TKR represents Tirukadaiyur, TGP Tharangampadi, CNP Chandrapadi, KCM Kottucherryedu, KJL Kilinjal medu, KRL Karaikkal, TRP T.R. Pattinam, NGR Nagore, NGP Nagapattinam, and VKN Velankanni.

littoral drift. As shown in the CM plot (Fig. 5c), the foreshore sediments falls under the uniform and graded suspension condition. During the NE monsoon, the predominant concentration of sediments is found to have segregated in PQ segment which has attested that the sediment samples of fluvial-marine process are influenced by the river discharge (Kulkarni et al., 2015). The convergent rays create maximum turbulence that leads to fluctuating size of the coarsest particles in the graded suspension (Rajaganapathi et al., 2013). Conversely, the sediments fall on overlying or uniform graded suspension (RS segment) during the SW monsoon. The divergence of waves decreases the turbulence, allowing the graded suspension to settle on the foreshore region. Hence, foreshore sediments appear as uniform suspension with well sorting nature during the SW monsoon.

3.2 Present results compared with *in situ* beach condition

The result of wave refraction and its impact on grain size and depositional environment is apparently correlated with the physical behavior of *in situ* beach and wave condition. During the NE

monsoon, waves break in the nearshore and cause significant widening of the surf zone and set a large amount of sediment in motion. Moreover, the beaches have attained flat terrace at low tide region by continuous erosion. This is due to the convergence of waves that leads to an increase the wave energy during the both uprush and backwash process. The energetic backwash lifts the foreshore sediments to form a series of sandbars at the surf zone (Joevivek et al., 2018a). From field observation, it could be noted that the foreshore sediments are mostly of fine grained heavy minerals (Joevivek et al., 2018b). Since, the less density of light mineral sand is washed by onshore-offshore wave processes; hence foreshore region enriched of fine-grained heavies (Fig. 1). During the SW monsoon, foreshore region attained continuous deposition. The divergence of waves leads to decrease the wave energy so that it leads to the littoral drift, produces sediment deposition. Hence, the uprush waves continuously supplied sediments to the foreshore and lift negligible amount of sediments while backrush (Fig. 1).

During the study period, the key parameter that is often con-

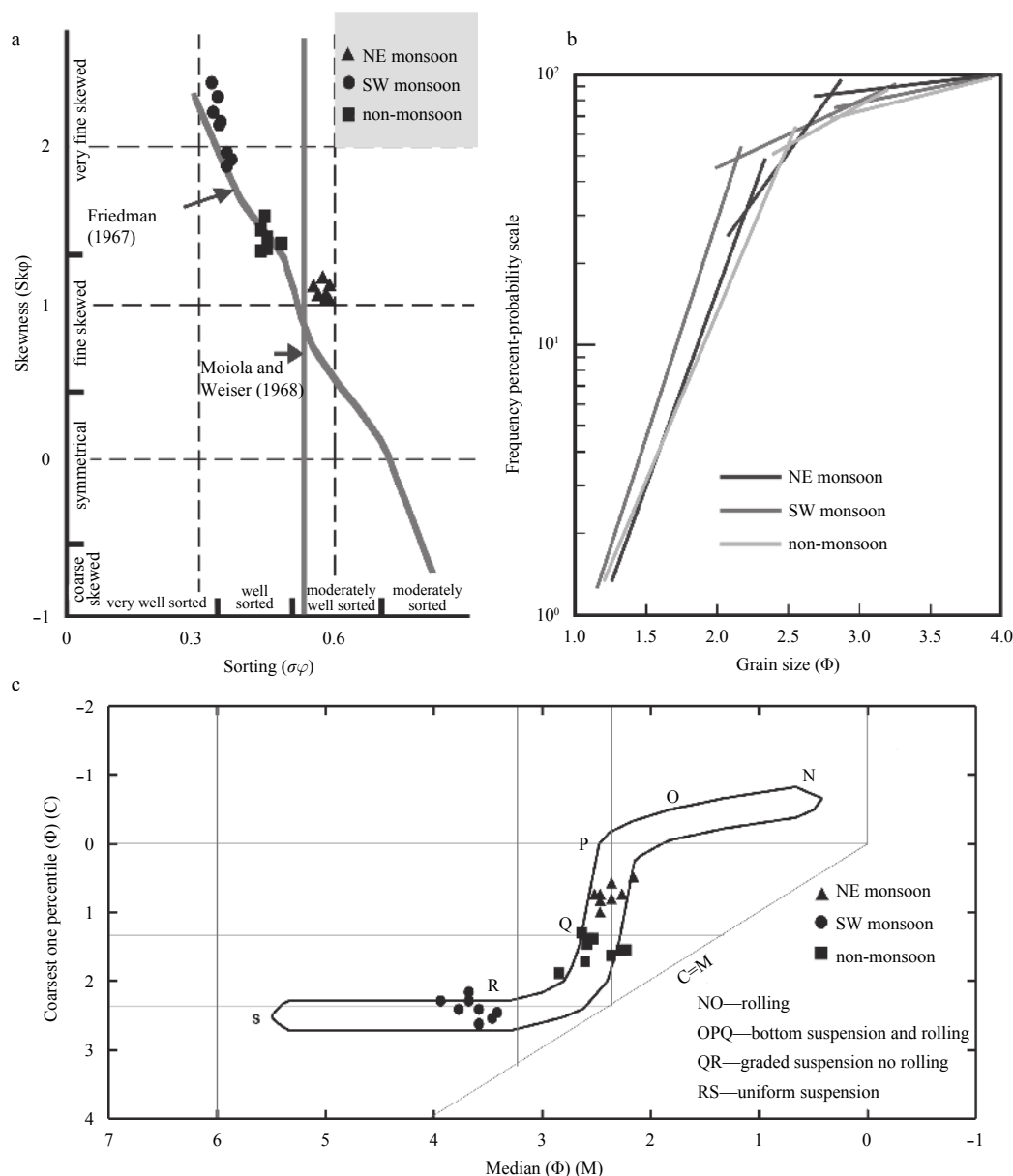


Fig. 5. Sediment depositional environment derived from the grain size distribution. a. Bi-variant plot classifies the sediment depositional environment, b. Visher plot demarcates the traction, saltation and suspension characteristics of the grain size, c. CM diagram shows the source of sediment population and depositional environment.

sidered for understanding the sediment distribution is the tidal fluctuation. Generally, the erosion process happens during the rising tide whereas the accretion process happens during the falling tide diurnally (Darsan, 2013). In the case of the micro-tidal beach systems, these short-term variations are considered to be insignificant and in case of assessing the long-term beach morphodynamics, tides are considered to be insignificant (Short, 1996). Nevertheless, the fluctuation in the tidal range is found to influence the shape, nature of the beach and the surf zone morphodynamics (Davis and Hayes, 1984; Short, 1991). From the above mentioned, it can be observed that the study area reveals the following conditions. During the southwest monsoon, it is found to be reflective beach state and mean spring tide range is relatively high (>1.0 m) (Table 1). The beach face appeared as steep slope, and a pronounced coarse step is usually found at the base of the swash zone fronted by a lower gradient. Whereas,

during the northeast monsoon, dissipative beach with low spring tide range (<0.7 m) showing spilling breakers and the low gradient beach face (see field photograph of Karaikkal in Fig. 1). Similarly, non-monsoon season shows spring tide range of <0.6 m which reflects the plunging and collapsing breakers and the transverse bar and rip beach system (Short, 1996). This physical phenomenon is consistent with the results obtained from the wave refraction, grain size and depositional environment. Overall, the NE monsoon waves erode the beach material and the SW and non-monsoon season waves rebuild it which results in stability of beach and nearshore condition over an annual cycle.

Acknowledgements

The first author is thankful to P. Vincent Jayaraj, George Udayaraj, Duraisamy and Pushparaj for their effective support during the field survey and Xavier Leema rose and Suganya Jenifer

for their help in developing the manuscript.

References

- Amrouni-Bouaziz O, Souissi R, Barusseau J P, et al. 2007. Grain-size and morphodynamical state of the bay-of-Mahdia shoreface (Tunisia). Contribution to the assessment of coastal sensitivity. *Geo-Eco-Marina*, No 13/2007, 5–19. <http://doi.org/10.5281/zenodo.57333>
- Angusamy N, Rajamanickam G V. 2006. Depositional environment of sediments along the southern coast of Tamil Nadu, India. *Oceanologia*, 48(1): 87–102
- Angusamy N, Udayaganesan P, Rajamanickam G V. 1998. Wave refraction pattern and its role in the redistribution of sediment along southern coast of Tamilnadu, India. *Indian Journal of Geo-Marine Sciences*, 27(2): 173–178
- Bird E C F. 2000. *Coastal Geomorphology: An Introduction*. New York: John Wiley & Sons, 322
- Blott S J, Pye K. 2001. GRADISTAT: A grain size distribution and statistics package for the analysis of unconsolidated sediments. *Earth Surface Processes and Landforms*, 26(11): 1237–1248, doi: [10.1002/esp.v26:11](https://doi.org/10.1002/esp.v26:11)
- Boggs S Jr. 2009. *Petrology of Sedimentary Rocks*. 2nd ed. Cambridge: Cambridge University Press, 600
- Briggs D J. 1977. *Sources and Methods in Geography: Sediments*. London: Butterworth and Co (Publ) Ltd, 55–86
- Chandramohan P, Nayak B U, Raju N S N. 1990. Wave tables for the Indian coast based on ship observations (1968–1986). National Institute of Oceanography, GOA, 312
- Darsan J. 2013. Beach morphological dynamics at Cocos Bay (Manzanilla), Trinidad. *Atlantic Geology*, 49: 151–168, doi: [10.4138/atageol.2013.008](https://doi.org/10.4138/atageol.2013.008)
- Davidson-Arnott R G D, Greenwood B. 2009. Waves and sediment transport in the nearshore Zone. In: Islaay F I, ed. *Coastal Zones and Estuaries (Volume I)*. Encyclopedia of Life Support Systems (EOLSS). Paris, France: UNESCO, Eolss Publishers, 43–60
- Davis R A, Hayes M O. 1984. What is a wave-dominated coast?. *Marine Geology*, 60(1–4): 313–329, doi: [10.1016/0025-3227\(84\)90155-5](https://doi.org/10.1016/0025-3227(84)90155-5)
- Duane D B. 1964. Significance of skewness in recent sediments, Western Pamlico Sound, North Carolina. *Journal of Sedimentary Research*, 34(4): 864–874
- Dube S K, Rao A D, Sinha P C, et al. 1997. Storm surge in the Bay of Bengal and Arabian Sea: The problem and its prediction. *Mausam*, 48(2): 283–304
- Dyer K R. 1986. *Coastal and Estuarine Sediment Dynamics*. New York: John Wiley and Sons Ltd, 342
- Folk R L, Robles R. 1964. Carbonate sands of Isla Perez, alacran reef complex, Yucatán. *The Journal of Geology*, 72(3): 255–292, doi: [10.1086/626986](https://doi.org/10.1086/626986)
- Friedman G M. 1961. Distinction between dune, beach, and river sands from their textural characteristics. *Journal of Sedimentary Research*, 31(4): 514–529
- Friedman G M. 1967. Dynamic processes and statistical parameters compared for size frequency distribution of beach and river sands. *Journal of Sedimentary Research*, 37(2): 327–354
- Galvin C J. 1968. Breaker type classification on three laboratory beaches. *Journal of Geophysical Research*, 73(12): 3651–3659, doi: [10.1029/JB073i012p03651](https://doi.org/10.1029/JB073i012p03651)
- Harrison W, Wilson W S. 1964. Development of A Method for Numerical Calculation of Wave Refraction. Washington: Coastal Engineering Research Centre
- Jing Lou, Massel S R. 1994. A combined refraction-diffraction-dissipation model of wave propagation. *Chinese Journal of Oceanology and Limnology*, 12(4): 361–371, doi: [10.1007/BF02850497](https://doi.org/10.1007/BF02850497)
- Joevivek V, Chandrasekar N. 2014. Seasonal impact on beach morphology and the status of heavy mineral deposition-central Tamil Nadu coast, India. *Journal of Earth System Science*, 123(1): 135–149, doi: [10.1007/s12040-013-0388-6](https://doi.org/10.1007/s12040-013-0388-6)
- Joevivek V, Chandrasekar N. 2016. ONWET: A simple integrated tool for beach morphology and wave dynamics analysis. *Marine Georesources & Geotechnology*, 34(6): 581–593, doi: [10.1080/1064119x.2015.1040904](https://doi.org/10.1080/1064119x.2015.1040904)
- Joevivek V, Chandrasekar N. 2017. Data on nearshore wave process and surficial beach deposits, central Tamil Nadu coast, India. *Data in Brief*, 13: 306–311, doi: [10.1016/j.dib.2017.05.052](https://doi.org/10.1016/j.dib.2017.05.052)
- Joevivek V, Chandrasekar N, Saravanan S, et al. 2018a. Spatial and temporal correlation between beach and wave processes: Implications for bar-berm sediment transition. *Frontiers of Earth Sciences*, 12(2): 349–360, doi: [10.1007/s11707-017-0655-y](https://doi.org/10.1007/s11707-017-0655-y)
- Joevivek V, Chandrasekar N, Shree P K. 2018b. Influence of porosity in quantitative analysis of heavy mineral placer deposits. *Oceanography & Fisheries Open Access Journal*, 6(3): 555689, doi: [10.19080/OFOAJ.2018.06.555689](https://doi.org/10.19080/OFOAJ.2018.06.555689)
- Kirby J T, Dalrymple R A. 1994. Combined Refraction/Diffraction Model REFDIF-1, Version 2.5. Technical Report No. CACR-94-22. Newark, DE: Center for Applied Coastal Research, Department of Civil Engineering, University of Delaware, 122
- Kulkarni S J, Deshbhandari P G, Jayappa K S. 2015. Seasonal variation in textural characteristics and sedimentary environments of beach sediments, Karnataka Coast, India. *Aquatic Procedia*, 4: 117–124, doi: [10.1016/j.aqpro.2015.02.017](https://doi.org/10.1016/j.aqpro.2015.02.017)
- Kunte P D, Wagle B G, Sugimori Y. 2001. Littoral transport studies along west coast of India—A review. *Indian Journal of Marine Sciences*, 30(2): 57–64
- López-Ruiz A, Solari S, Ortega-Sánchez M, et al. 2015. A simple approximation for wave refraction—Application to the assessment of the nearshore wave directionality. *Ocean Modelling*, 96: 324–333, doi: [10.1016/j.ocemod.2015.09.007](https://doi.org/10.1016/j.ocemod.2015.09.007)
- Martins L R. 1965. Significance of skewness and kurtosis in environmental interpretation. *Journal of Sedimentary Research*, 35(3): 768–770, doi: [10.1306/74D7135C-2B21-11D7-8648000102C1865D](https://doi.org/10.1306/74D7135C-2B21-11D7-8648000102C1865D)
- Masselink G, Puleo J A. 2006. Swash-zone morphodynamics. *Continental Shelf Research*, 26(5): 661–680, doi: [10.1016/j.csr.2006.01.015](https://doi.org/10.1016/j.csr.2006.01.015)
- Mathiesen M. 1987. Wave refraction by a current whirl. *Journal of Geophysical Research*, 92(C4): 3905–3912, doi: [10.1029/JC092iC04p03905](https://doi.org/10.1029/JC092iC04p03905)
- Moiola R J, Weiser D. 1968. Textural parameters: An evaluation. *Journal of Sedimentary Research*, 38(1): 45–53
- Munk W H, Traylor M A. 1947. Refraction of ocean waves; A process linking underwater topography to beach erosion. *The Journal of Geology*, 55(1): 1–26
- Orr T E. 1969. Numerical calculation of wave refraction by digital computer. Texas: Texas A&M University
- Passega R. 1964. Grain size representation by CM patterns as a geologic tool. *Journal of Sedimentary Research*, 34(4): 830–847, doi: [10.1306/74D711A4-2B21-11D7-8648000102C1865D](https://doi.org/10.1306/74D711A4-2B21-11D7-8648000102C1865D)
- Rajaganapathi V C, Jitheskumar N, Sundararajan M, et al. 2013. Grain size analysis and characterization of sedimentary environment along Thiruchendur coast, Tamilnadu, India. *Arabian Journal of Geosciences*, 6(12): 4717–4728, doi: [10.1007/s12517-012-0709-0](https://doi.org/10.1007/s12517-012-0709-0)
- Saravanan S, Chandrasekar N. 2015. Wave Refraction Pattern and Littoral Sediment Transport along the SE Tamilnadu Coast, India. *Journal of Coastal Research*, 31(2): 291–298
- Segtnan O H. 2014. Wave refraction analyses at the coast of norway for offshore applications. *Energy Procedia*, 53: 193–201, doi: [10.1016/j.egypro.2014.07.228](https://doi.org/10.1016/j.egypro.2014.07.228)
- Shepard F P, Inman D L. 1950. Nearshore water circulation related to bottom topography and wave refraction. *Eos, Transactions American Geophysical Union*, 31(2): 196–212, doi: [10.1029/TR031i002p00196](https://doi.org/10.1029/TR031i002p00196)
- Short A D. 1991. Macro-meso tidal beach morphodynamics: An overview. *Journal of Coastal Research*, 7(2): 417–436
- Short A D. 1996. The role of wave height, period, slope, tide range and embaymentisation in beach classifications: a review. *Revista Chilena de Historia Natural*, 69(4): 589–604
- Short A D. 2006. Australian beach systems-nature and distribution. *Journal of Coastal Research*, 22(1): 11–27
- Skovgaard O, Bertelsen J A, Jonsson I G. 1975. Computation of wave heights due to refraction and friction. *Journal of the Waterways*,

- Harbors and Coastal Engineering Division, 101(1): 15–32
- Soomere T, Kask A, Kask J, et al. 2008. Modelling of wave climate and sediment transport patterns at a tideless embayed beach, Pirita Beach, Estonia. *Journal of Marine Systems*, 74: S133–S146, doi: [10.1016/j.jmarsys.2008.03.024](https://doi.org/10.1016/j.jmarsys.2008.03.024)
- Visher G S. 1969. Grain-size distributions and depositional processes. *Journal of Sedimentary Petrology*, 39(3): 1074–1106
- Wentworth C K. 1922. A scale of grade and class terms for clastic sediments. *The Journal of Geology*, 30(5): 377–392, doi: [10.1086/622910](https://doi.org/10.1086/622910)
- Wright L D, Short A D. 1984. Morphodynamic variability of surf zones and beaches: A synthesis. *Marine Geology*, 56(1–4): 93–118, doi: [10.1016/0025-3227\(84\)90008-2](https://doi.org/10.1016/0025-3227(84)90008-2)
- Yates M L, Guza R T, O'Reilly W C, et al. 2011. Equilibrium shoreline response of a high wave energy beach. *Journal of Geophysical Research*, 116(C4): C04014